Measurement and theoretical modelling of the damping rate of medium-n TAEs in JET

D.Testa[1], T.Panis[1], A.Fasoli[1], P.Blanchard[1,2], H.Carfantan[3], A.Goodyear[4], N.Mellet[1,5], S.E.Sharapov[4], D.Spong[6], JET-EFDA contributors

JET-EFDA, Culham Science Centre, OX14 3DB, Abingdon, UK

[1] Centre de Recherches en Physique des Plasmas, Ecole Polytechnique Fédérale de Lausanne, Association EURATOM – Confédération Suisse, CH
[2] JET-EFDA Close Support Unit, Culham Science Centre, Abingdon, UK
[3] Laboratoire d'Astrophysique de Toulouse – Tarbes, Université de Toulouse – CNRS, FR
[4] Culham Center for Fusion Energy, Culham Science Centre, Abingdon, UK
[5] Association Euratom CEA, Cadarache, Saint-Paul-lez-Durance, France
[6] Oak Ridge National Laboratory, Fusion Energy Theory Group, Oak Ridge, USA

EFDA EUROPEAN FUSION DEVELOPMENT AGREEMENT JET EPFL CRPP

Alfvén Eigenmode Active Diagnostics

Aim: address physics of mode damping, identify modes most prone to instability in different burning plasma scenarios, and parameters to control stability

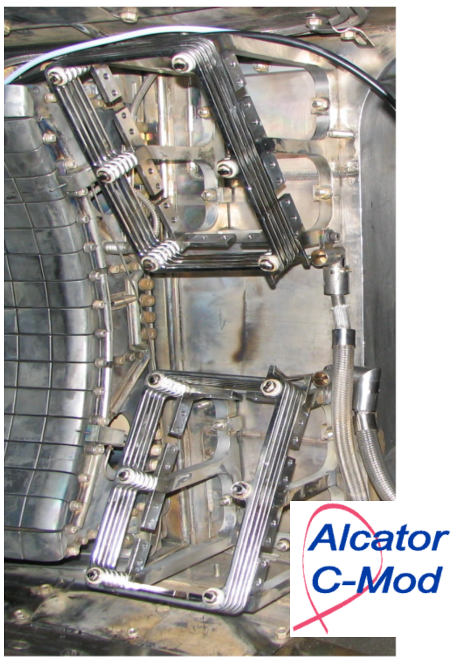

high field & density, $T_e \sim T_i$

EFDA EUROPEAN FUSION DEVELOPMENT AGREEMENT JET

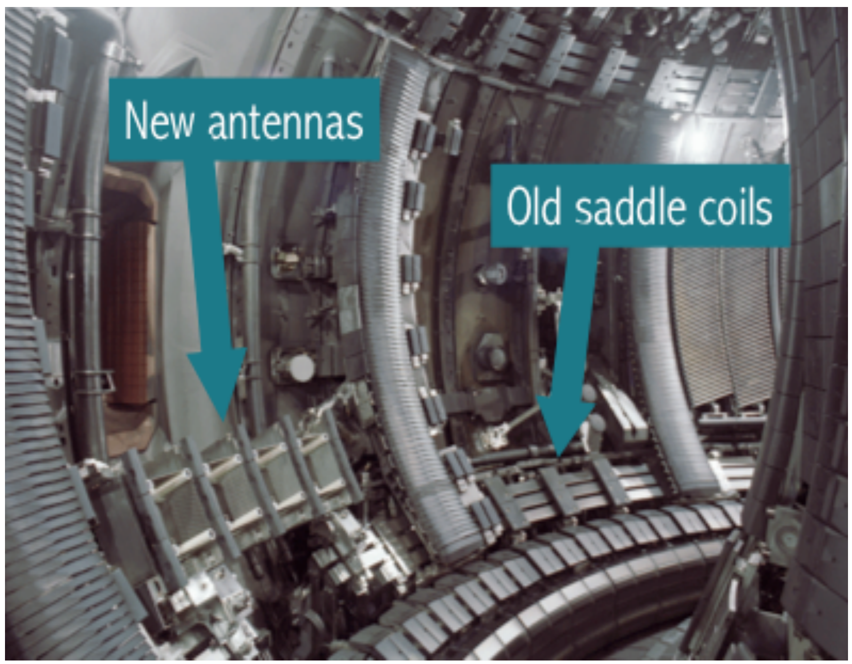

ITER-relevance for size and shape scaling, scenarios

MAST

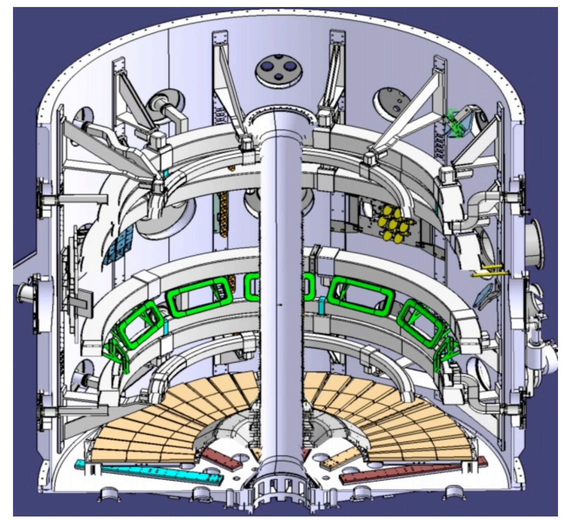

tight aspect ratio,
broad range of β

JET AE antennas

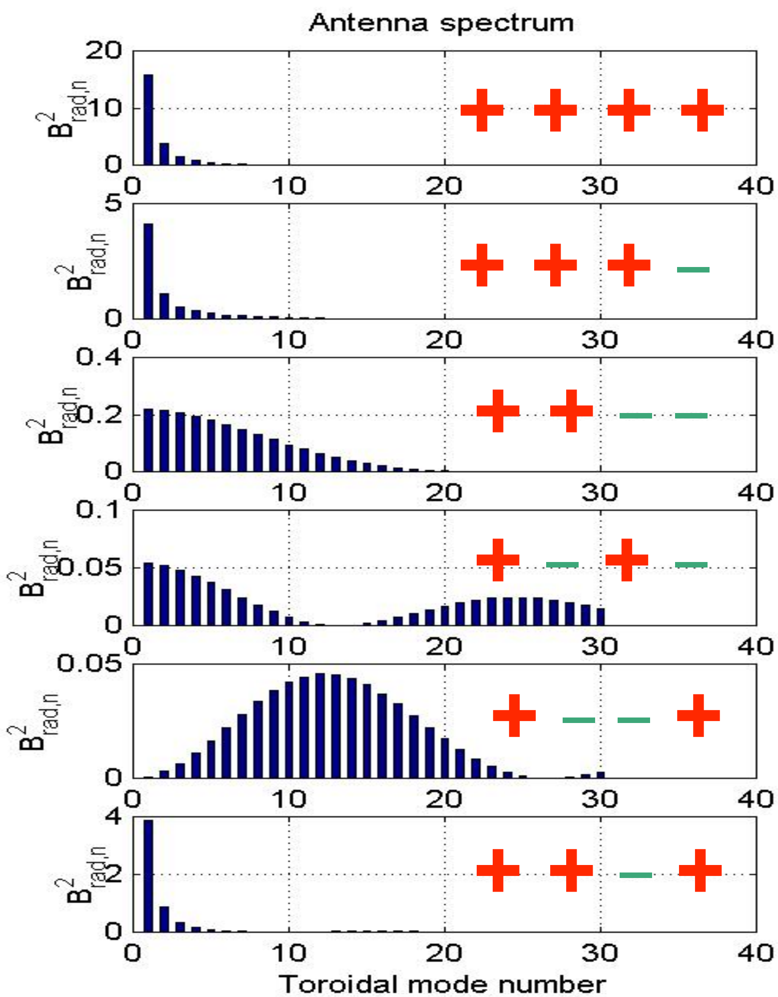

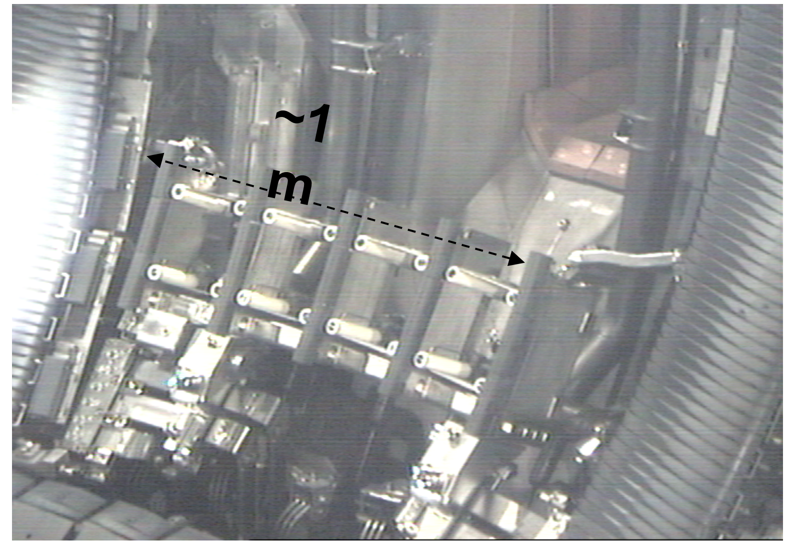

Oct 8
(2005)

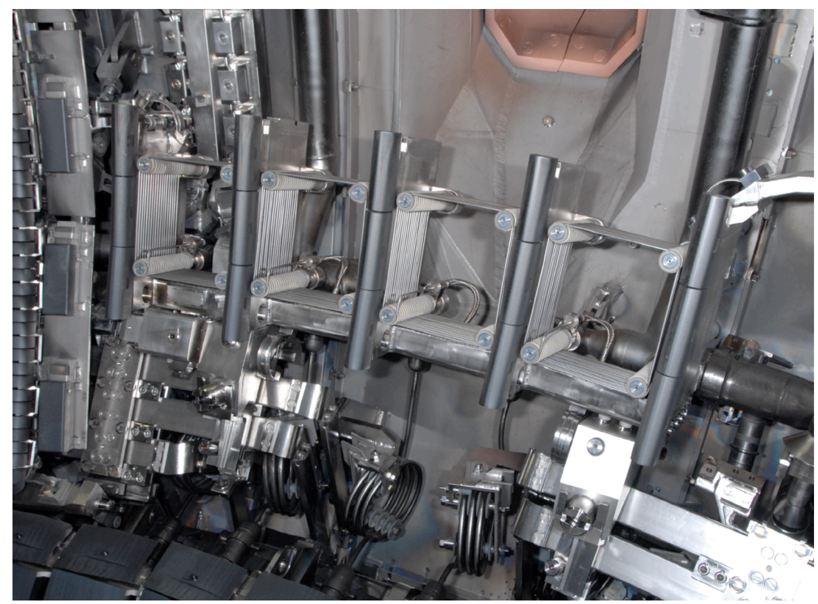

Oct 4
(2007)

Unique capability: real-time tracking to follow mode evolution as plasma parameters change

Ex. of γ/ω measurements for n=7 TAE

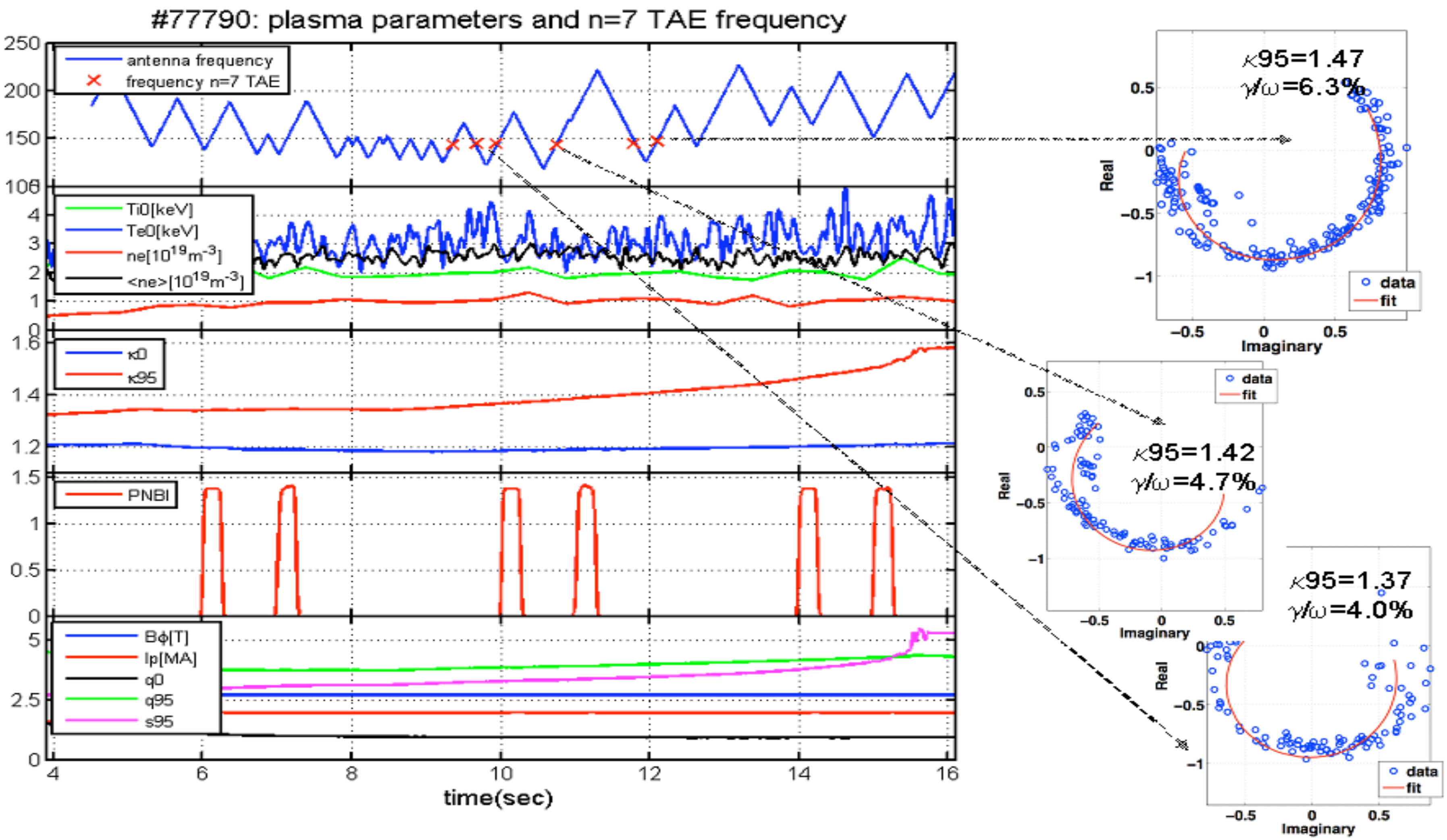

Note: in the absence of fast ion drive, γ/ω is the mode damping rate

Outline

- Real-time mode decomposition and tracking

- Measurements of TAE damping rate
  - Database and trends
    - Parameter ranges in which measurements are possible
    - Parametric dependencies for dominant damping mechanism(s)
  - Individual discharge analysis
    - Essential for detailed comparisons with theory
    - Ex.: modeling of n=3 TAEs using LEMan, CASTOR, TAEFL

- Outlook: Active diagnostic upgrade

Real-time detection and tracking of individual n-components

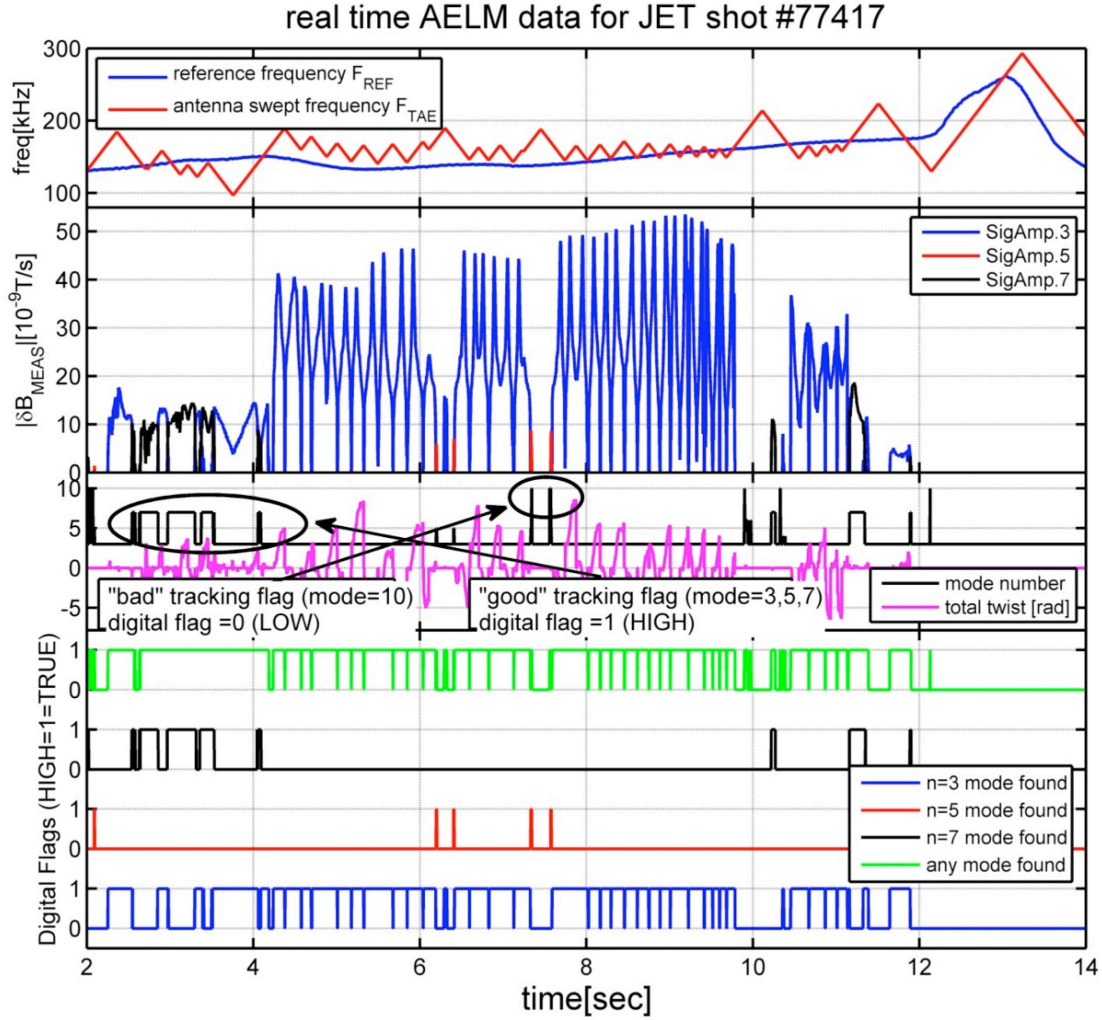

- Antenna spectrum contains several frequency-degenerate modes
- Discrimination of n's done in real-time using sparse representation method (SparSpec)
- Computation within 850μs

Example

- Antenna configuration to drive odd modes (3<|n|<11)
- n=3 mode dominates
- Weaker n=5, 7 modes

Post-pulse analysis (no time limitations for calculation) reveals entire set of modes

For modes also measured in real-time the difference in f, γ/ω and n are within 20%

AE damping database
Range of plasma parameters

plasma parameter	min	max
I_p (MA)	0.93	2.58
B_0 (T)	1.87	3.37
q_0	0.72	2.70
q_{95}	2.63	6.56
s_{95}	2.21	4.73
κ_{95}	1.25	1.71
δ_u	-0.02	0.34
δ_l	-0.01	0.33
ROG (m)	0.01	0.12
β_N	0.15	0.54
β_t (%)	0.06	0.46
β_p	0.13	0.25
n_{e0} (10^{19} m^{-3})	~1	~3
T_{e0} (keV)	~1	~4

~10000 TAE damping rate measurements in ohmic plasmas

AE damping database
Looking for correlations

plasma quantity	$\|n\|$						
	1	2	3	4	5	6	7
q_0	-0.05	-0.00	-0.30	-0.17	-0.05	0.09	-0.42
q_{95}	-0.05	-0.03	-0.18	-0.06	0.11	0.04	**-0.57**
$q_{95} - q_0$	-0.05	-0.05	-0.09	0.04	0.20	0.02	**-0.52**
q_{95}/q_0	0.14	-0.04	0.24	0.20	0.16	-0.21	0.11
s_{95}	**0.60**	0.22	0.31	0.29	0.09	-0.28	0.02
κ_{95}	**0.49**	0.19	0.22	0.25	-0.13	-0.26	-0.18
δ_u	0.36	0.12	0.10	0.21	0.07	-0.39	-0.05
δ_l	0.30	0.22	0.04	0.29	0.20	-0.29	-0.13
I_p	-0.40	-0.04	-0.00	0.12	-0.24	-0.14	-0.24
β_N	0.22	0.04	0.32	0.13	0.01	0.04	0.38
β_t	0.28	0.07	0.38	0.17	-0.09	0.02	**0.50**
β_p	0.09	-0.07	0.04	0.09	0.21	-0.03	-0.09
B_0	**-0.69**	-0.09	-0.34	-0.07	-0.24	-0.06	**-0.51**
ROG	-0.01	-0.07	0.03	0.21	-0.05	0.05	0.12
T_{e0}	-0.20	-0.01	-0.13	0.09	-0.38	0.01	-0.10
n_{e0}	-0.16	-0.09	-0.02	-0.07	-0.23	-0.27	-0.29
λ	**0.75**	0.18	0.23	0.29	-0.05	0.05	0.05

Correlation coefficient

$$r = \frac{\sum_{i=1}^{N}(x_i - \bar{x})(y_i - \bar{y})}{\sqrt{\sum_{i=1}^{N}(x_i - \bar{x})^2 \sum_{i=1}^{N}(y_i - \bar{y})^2}}$$

AE damping database
Looking for correlations

plasma quantity	$\|n\|$						
	1	2	3	4	5	6	7
q_0	-0.05	-0.00	-0.30	-0.17	-0.05	0.09	-0.42
q_{95}	-0.05	-0.03	-0.18	-0.06	0.11	0.04	**-0.57**
$q_{95} - q_0$	-0.05	-0.05	-0.09	0.04	0.20	0.02	**-0.52**
q_{95}/q_0	0.14	-0.04	0.24	0.20	0.16	-0.21	0.11
s_{95}	**0.60**	0.22	0.31	0.29	0.09	-0.28	0.02
κ_{95}	**0.49**	0.19	0.22	0.25	-0.13	-0.26	-0.18
δ_u	0.36	0.12	0.10	0.21	0.07	-0.39	-0.05
δ_l	0.30	0.22	0.04	0.29	0.20	-0.29	-0.13
I_p	-0.40	-0.04	-0.00	0.12	-0.24	-0.14	-0.24
β_N	0.22	0.04	0.32	0.13	0.01	0.04	0.38
β_t	0.28	0.07	0.38	0.17	-0.09	0.02	**0.50**
β_p	0.09	-0.07	0.04	0.09	0.21	-0.03	-0.09
B_0	**-0.69**	-0.09	-0.34	-0.07	-0.24	-0.06	**-0.51**
ROG	-0.01	-0.07	0.03	0.21	-0.05	0.05	0.12
T_{e0}	-0.20	-0.01	-0.13	0.09	-0.38	0.01	-0.10
n_{e0}	-0.16	-0.09	-0.02	-0.07	-0.23	-0.27	-0.29
λ	**0.75**	0.18	0.23	0.29	-0.05	0.05	0.05

Correlation coefficient

$$r = \frac{\sum_{i=1}^{N}(x_i - \bar{x})(y_i - \bar{y})}{\sqrt{\sum_{i=1}^{N}(x_i - \bar{x})^2 \sum_{i=1}^{N}(y_i - \bar{y})^2}}$$

γ/ω for 1<|n|<7 TAEs vs. q_0

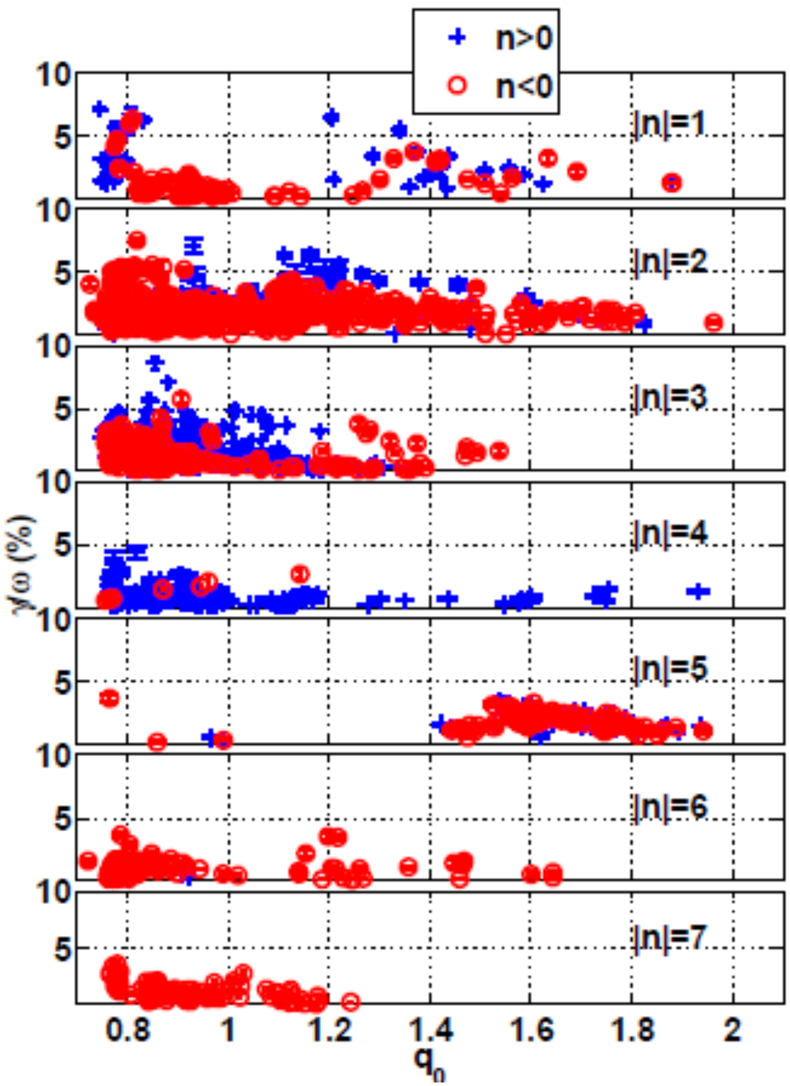

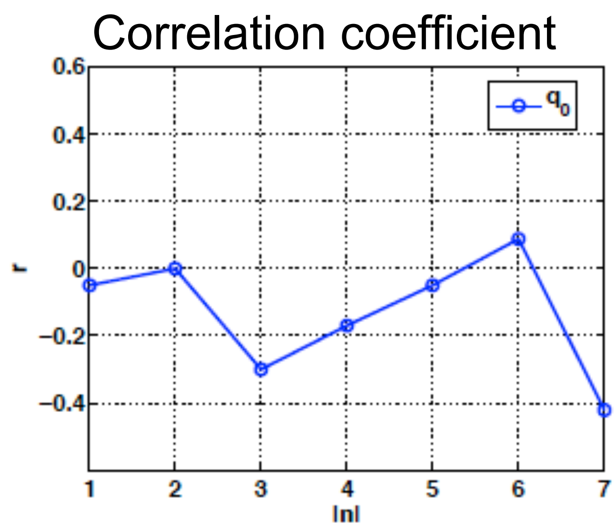

- No clear general trend in $\gamma/\omega=f(q_0)$
- *Try selection of shots with similar q_{95} and varying q_0 during q-profile relaxation*

γ/ω for 1<|n|<7 TAEs vs. q_0
Selection of shots with fixed q_{95}

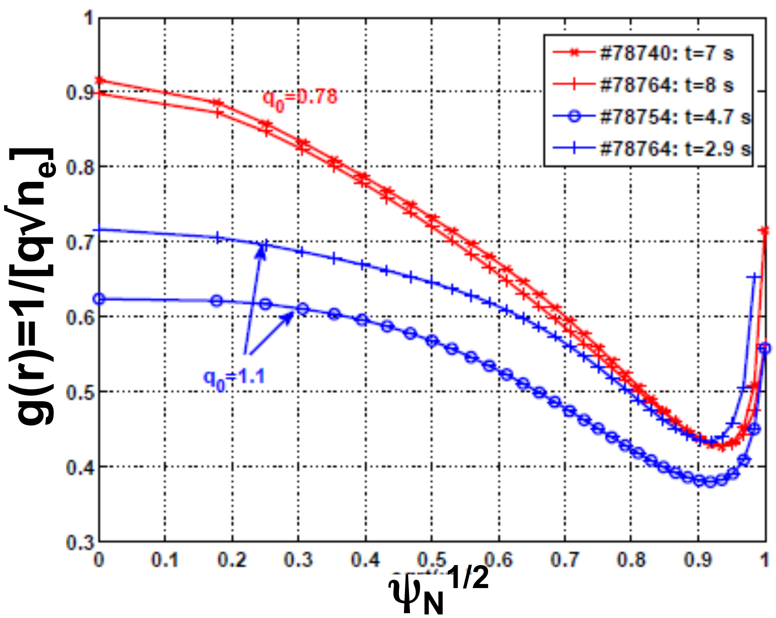

- For same q_{95}, Alfvén continuum gaps get less and less aligned as q-profile relaxes (q_0 decreases)
- This effect is quantified by $1/[q\sqrt{n_e}(r)]$
- Estimate of continuum damping

γ/ω for $1<|n|<7$ TAEs vs. q_0
Selection of shots with fixed q_{95}

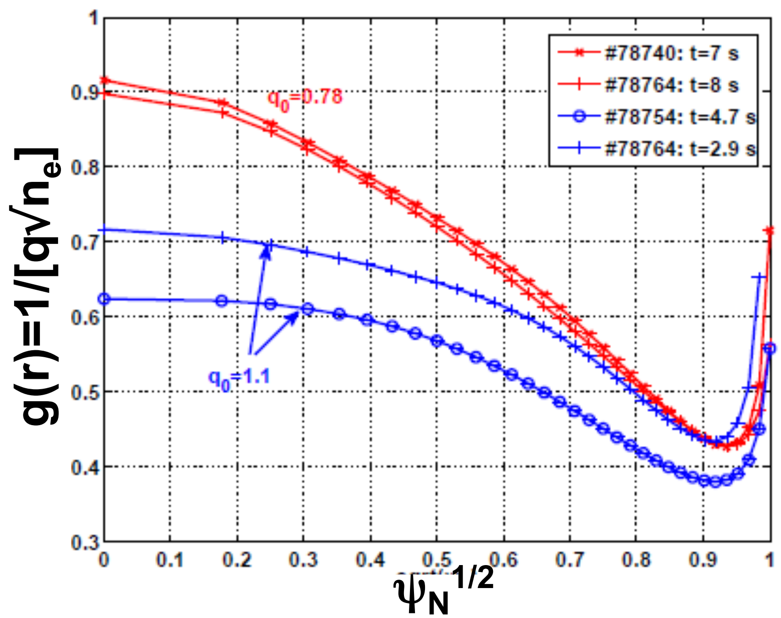

- For same q_{95}, Alfvén continuum gaps get less and less aligned as q-profile relaxes (q_0 decreases)
- This effect is quantified by $1/[q\sqrt{n_e}(r)]$
- Estimate of continuum damping

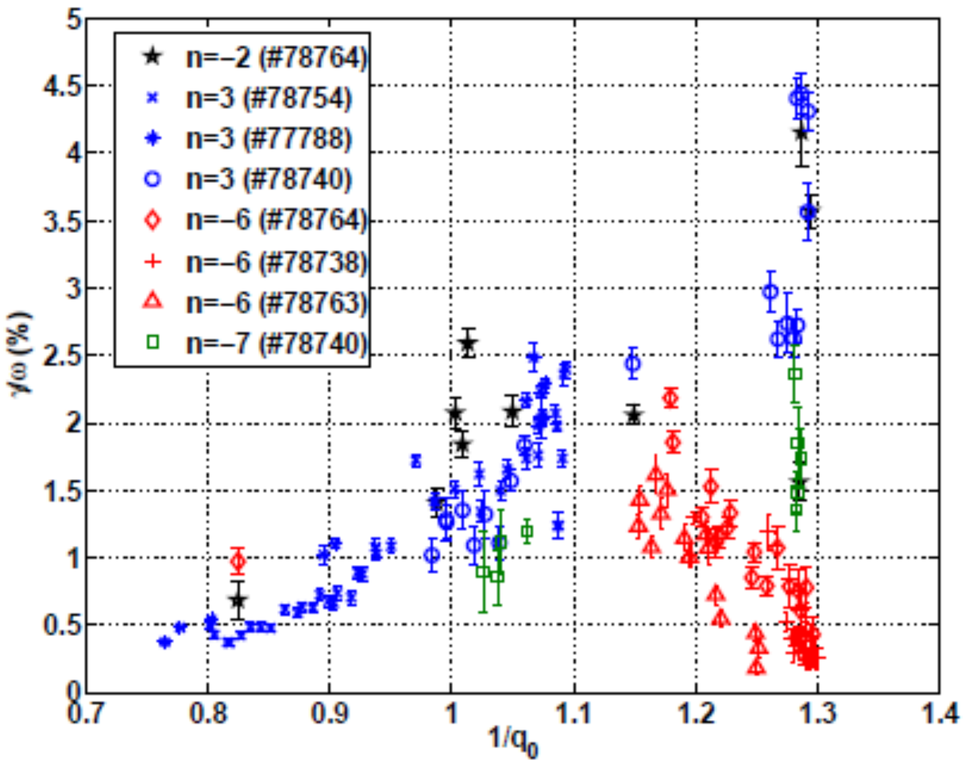

- Evidence for difference between n-ranges: continuum and radiative damping less effective as n increases

γ/ω for 1<|n|<7 TAEs vs. λ

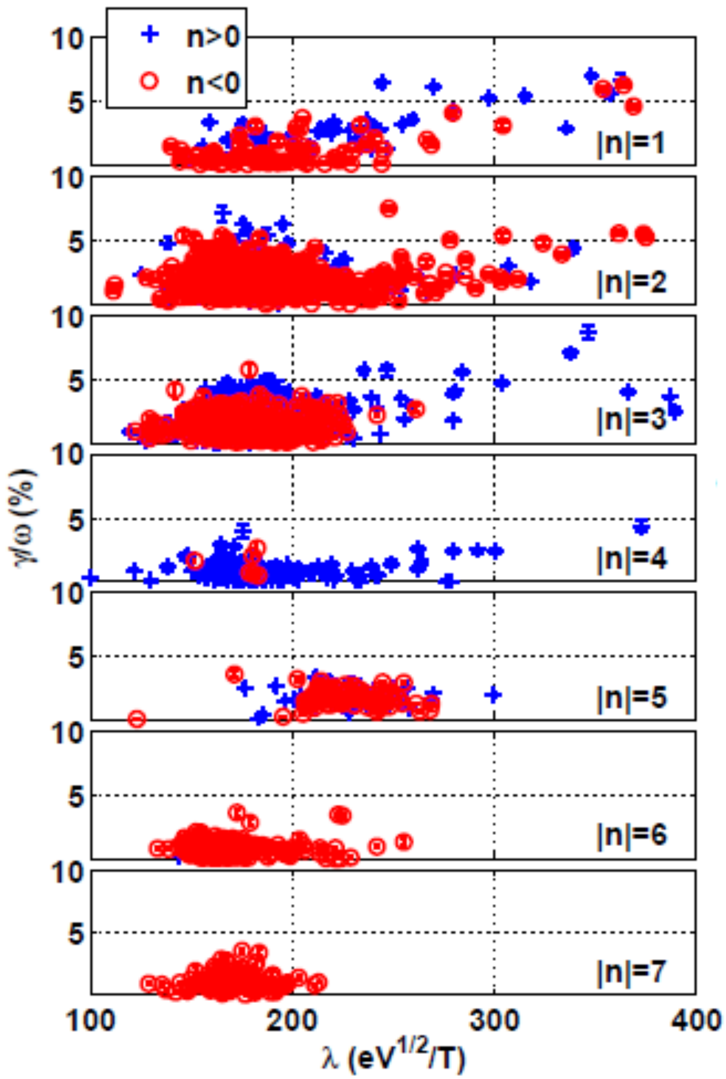

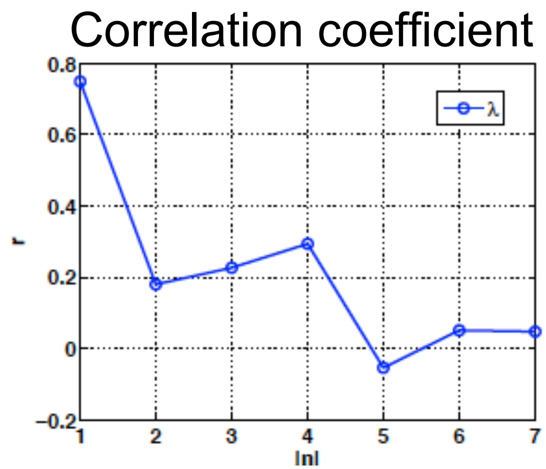

- Non-ideal parameter $\lambda \propto q_{95} s_{95} \sqrt{T_{e0}}/B_0$ provides estimate of radiative damping
- Clear trend for |n|=1: $\gamma/\omega_{|n|=1} \propto \lambda$
- Similar trend for 2≤|n|≤4, only for large λ
- No clear trend for |n|≥5

Edge shape effect on TAE damping

Old, saddle coil driven n=1 measurements indicated a clear trend

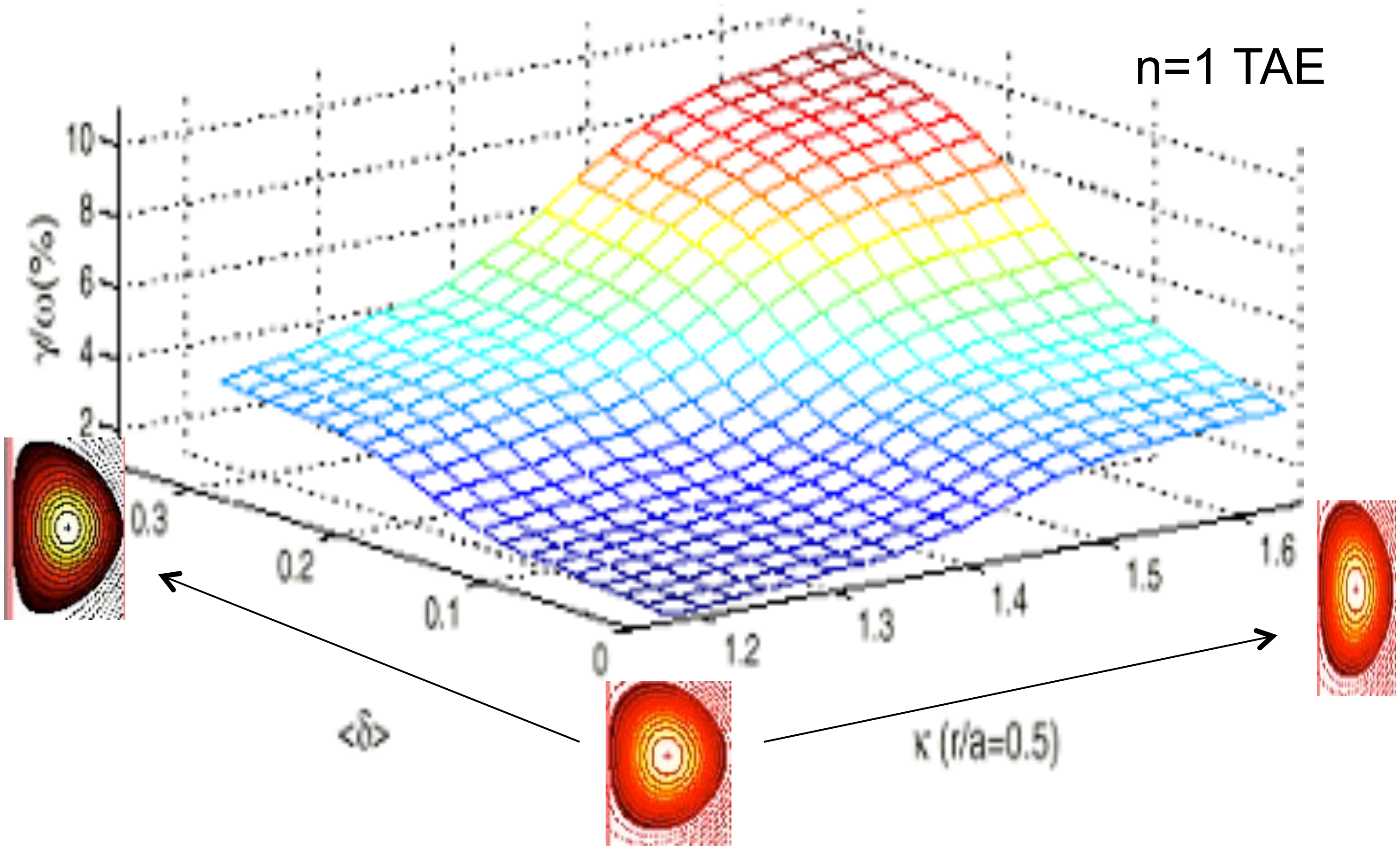

γ/ω for 1<|n|<7 TAEs vs. edge shape

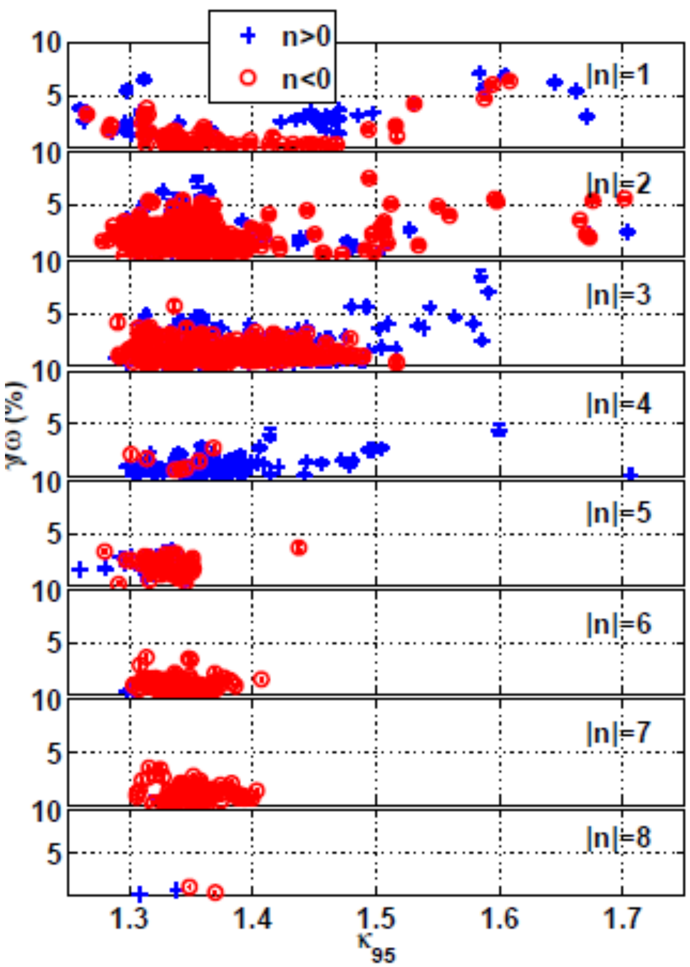

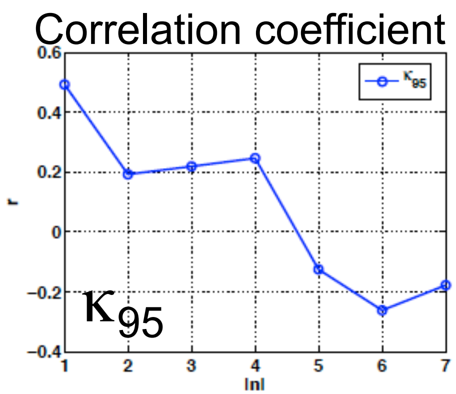

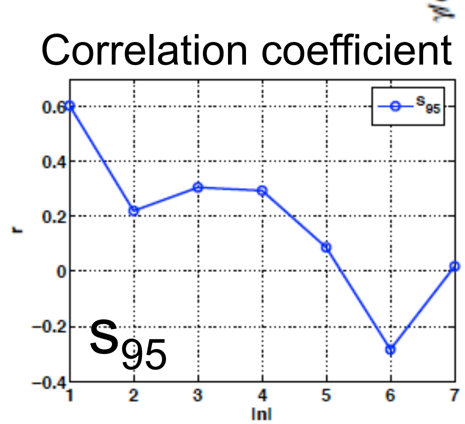

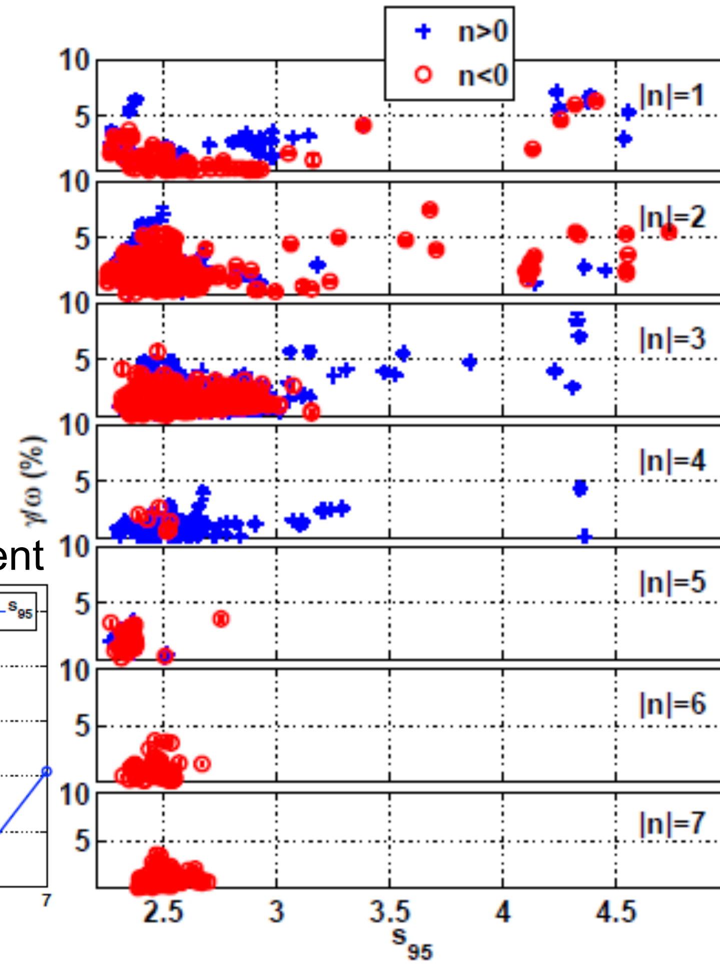

- No data points for which γ/ω<7% for large values of κ_{95} and s_{95}
- Clear trend only visible in general for low-n
- To assess effect for medium-n a single shot approach is necessary

γ/ω for |n|=3, 7 TAEs vs. edge shape Single shot approach

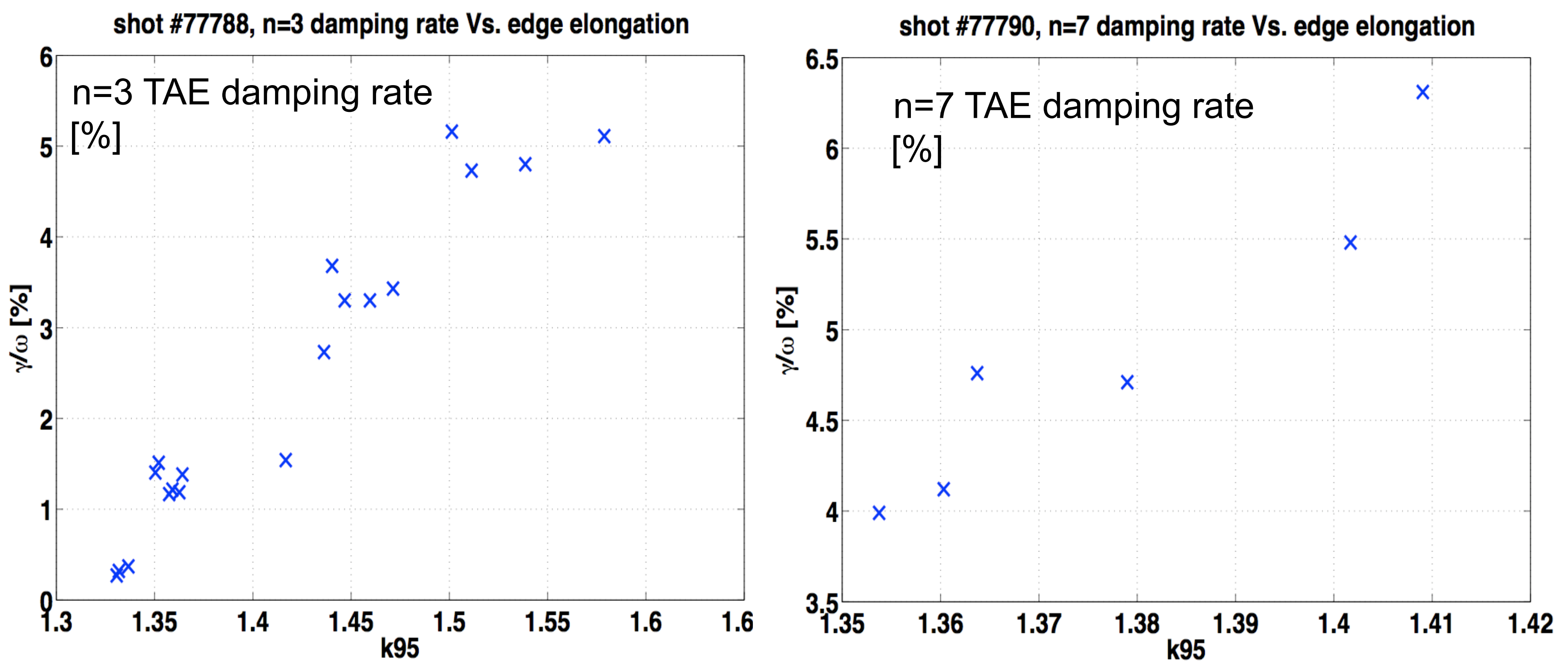

- In single shot, single-n measurements, edge elongation leads to increase in damping
- Why is this trend not visible in database?
- *Disentangle two dependences, e.g. q-profile and edge shape in specific experiment*

Disentangling influence of edge shape and q-profile on n=3 TAE damping

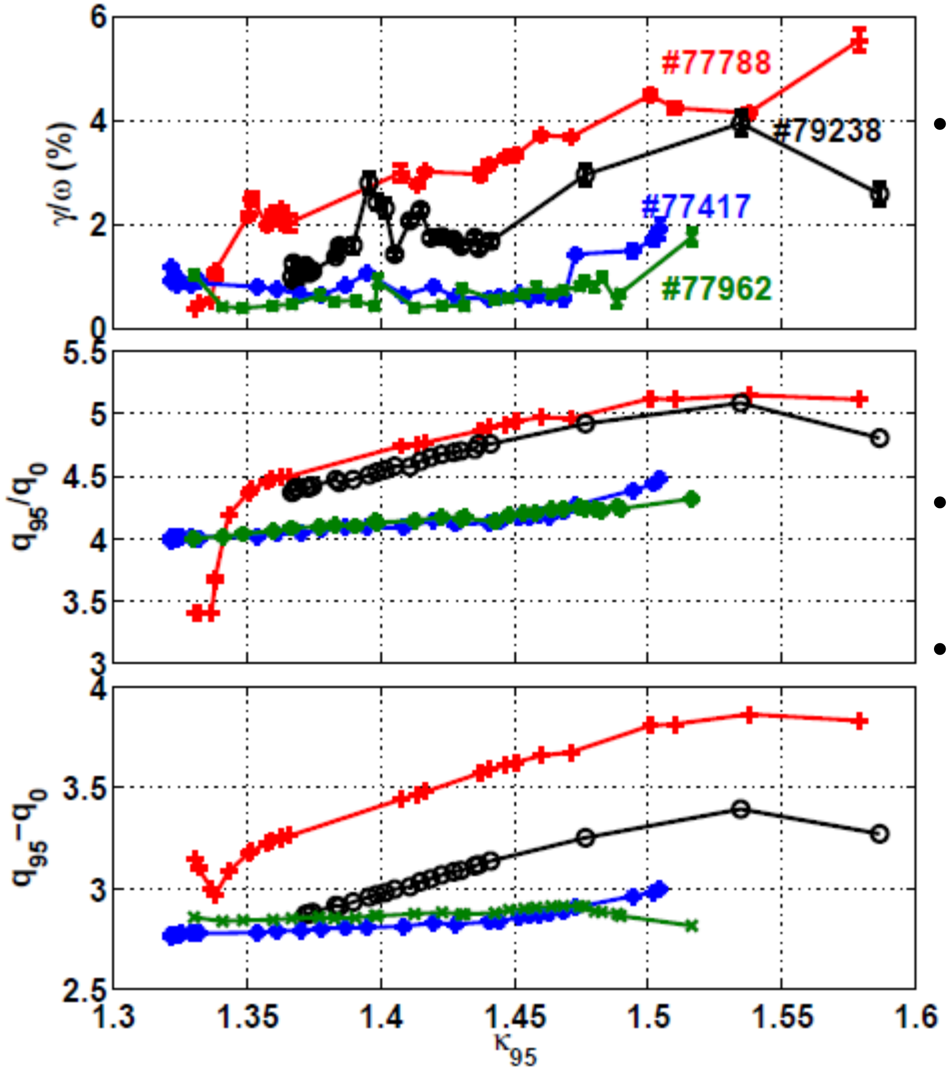

- Differences in γ/ω for same κ_{95} in different discharges seem related to 'span' of q-profile, quantified by q_{95}/q_0 and q_{95}-q_0 (proportional to number of poloidal harmonics)
- Damping increases with q_{95}/q_0 and q_{95}-q_0
- Trend consistent with electron Landau damping scaling $(\gamma/\omega)_{ELD} \propto n^2(q_{95}-q_0)^2$

n=3 TAE damping: modeling shape effect

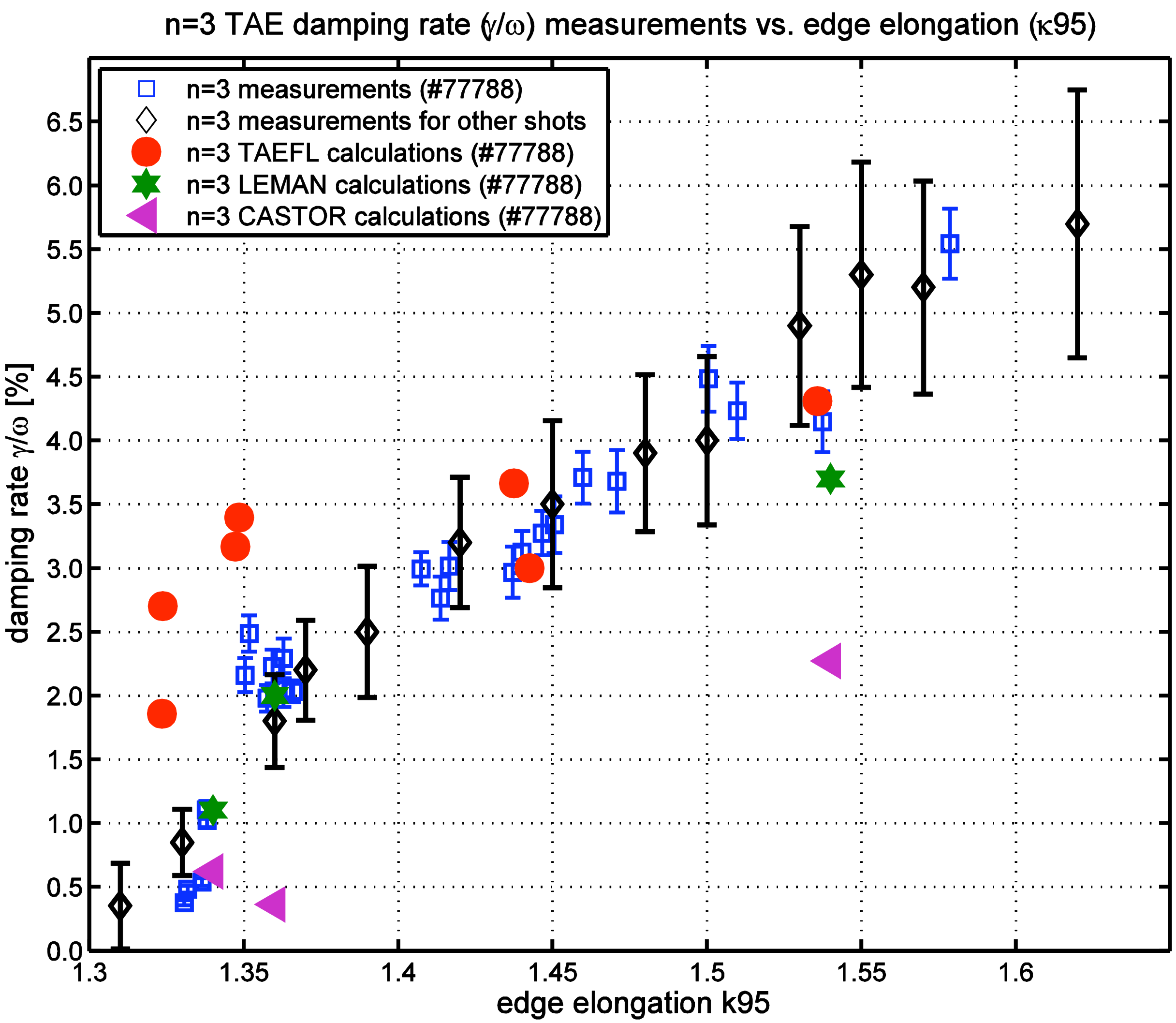

- **CASTOR**: fluid
  - Large discrepancies with data
- **TAEFL**: gyro-fluid
  - γ/ω extrapolated back from marginal stability threshold for fast-ion driven modes
  - Good agreement with data, important to test validity of modeling approach
- **LEMan**: gyro-kinetic
  - Good agreement with data
  - Electron Landau damping of mode converted kinetic AW
  - *Note: good agreement was also found in comparisons with gyro-kinetic code LIGKA*

Summary

- JET AE exciter drives and detects real-time selected spectrum of medium-n Aes
- Damping measurements database suggests some global trends for damping rates
- Individual discharge and n analysis is needed to disentangle complex dependences of γ/ω on various parameters and profiles
- Agreement with numerical codes based on gyro-kinetic or gyro-fluid models has reached quantitative level

Limitations of present AE system

- Coupling
  - Even with optimal matching and coils from both antennas, with one amplifier (I_{max}~5A), core amplitudes are very small
    - ~0.05mG/1A in the plasma core for modes with n~7-15
  - Tracking is difficult in the presence of noise (e.g. during strong additional heating) and if LCFS is distant from antennas
  - Mode identification requires sophisticated n-detection algorithms
- Mode selection
  - Wide spectrum; plasma preferentially selects low-n's

n distribution of damping rate measurements

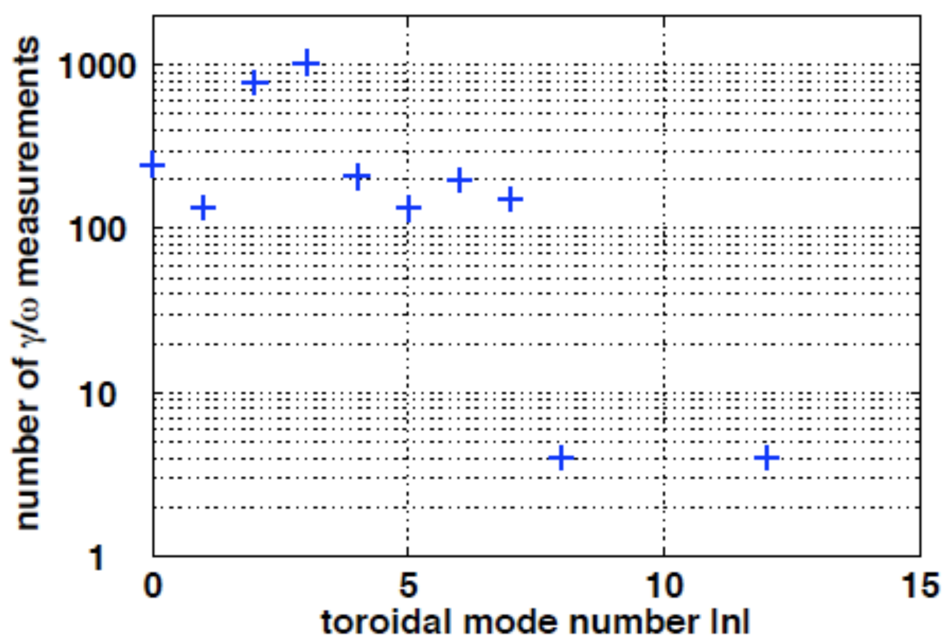

Upgrade to 8 independent amplifiers

- Maximize antenna currents within feed-through limits (25A)
- Better definition of antenna spectrum
  - Gain in single mode excitation by ~ factor of 4
  - More balanced distribution of currents without transformer coupling
- Arbitrary phasing
  - Definition of sign of n (traveling wave): identification of fast ion contribution
  - Simultaneous excitation of selected modes (different n's or frequencies)
    - Stronger constraint on theory simulations for ITER extrapolation
    - Multi-point diagnostic applications
      - $q(r_1, r_2,..)$, $A_{EFF}(r_1, r_2,..)$, $\omega_{TOR}(r_1, r_2,..)$
- Test of burn control ideas
  - Real time control of fast ion stability by mode tracking

the Sparse Representation Method

SparSpec minimizes the L1-norm penalized criterion:

$$J(x) = \tfrac{1}{2}\left\|\mathbf{y} - W\mathbf{x}\right\|^2 + \lambda \sum_{k=-K}^{K} \left|x_k\right|_{L1}$$

y: vector of data taken at time t_k [≡ position ϕ_k]
W: spectral window $\exp(i2\pi t_k f_n)$ [≡ $\exp(i2\pi\phi_k n)$]
x: vector of (I,Q) signals for frequencies f_n
λ: parameter fixed to obtain a satisfactory sparse solution ➔ **penalty criterion for invoking more modes to find adequate solution**
λ can be fixed a-priori from known noise variance

- the sparse signal representation method is ideally suited for mode number analysis in fusion plasmas:
  - specifically designed for un-evenly distribution of sensors
  - allowable mode numbers are discretized: |n| = 0, ±1, ±2, ±3…
  - large (n,m)-range, number of modes not assumed a priori
  - amplitude and phase equally important for fitting algorithm
  - no need for a-posteriori tresholding to discriminate between solutions as λ-penalty determined a-priori from knowledge of noise variance
  - very efficient, very fast convergence ➔ ideal for real-time applications
  - **now implemented and fully validated in JET real-time and post-pulse mode tracking algorithm for stable Alfvén Eigenmodes**
  - **accuracy ➔ need correct interpretation of the spectral window**

γ/ω measurements for medium-n AEs: data available for theory comparisons

- database compiled of $\gamma/\omega(n)$ as function of plasma parameters and configurations for individual mode numbers
  - in excess of 10'000 individual $\gamma/\omega(n)$ measurements already analyzed
  - in excess of 60 individual discharges already analyzed
  - various dedicated scans in plasma parameters have been run:
    - elongation scan during ohmic phase, $1.25<\kappa95<1.65$ without IRCF
      - add ICRF with PRF=2MW and PRF=3MW, different phasing (dipole and +/-90)
      - add PRF modulations 2MW +1MW/300ms, different phasing (dipole and +/-90)
    - ohmic Bfield/ne scan, change RF deposition profile and edge continuum
      - add PRF with power ramp-up to 4.5MW, different phasing (dipole and +/-90)
- damping rate as function of plasma isotope composition and ion Larmor radius
- damping rate for medium-n (n=3-7) TAEs at ICRF power switch off with constant plasma parameters
  - direct measurement of MeV-ions drive to the modes?
- effect of ripple in the magnetic field medium-n (n=3-7) TAEs with/out fast ions:
  - fast ion losses (resonant NBI ions with $V_{||}\sim V_A/3$), affecting drive for the modes?
  - change density scale length at plasma edge, affecting the continuum damping?